

## Magnetic and resonance properties of $\text{LiCu}_2\text{O}_2$ single crystals

A. M. Vorotynov, A. I. Pankrats, G. A. Petrakovskii,<sup>\*</sup> and K. A. Sablina

*L. V. Kirenskiĭ Institute of Physics, Siberian Branch of the Russian Academy of Sciences, 660036 Krasnoyarsk, Russia*

W. Paszkowicz and H. Szymczak

*Institute of Physics, Polish Academy of Sciences, 02-668 Warsaw, Poland*  
(Submitted 31 October 1997)

Zh. Ėksp. Teor. Fiz. **113**, 1866–1876 (May 1998)

We study the structural, magnetic, and resonance properties of  $\text{LiCu}_2\text{O}_2$  single crystals grown by the spontaneous crystallization method. The data are interpreted on the assumption that the crystalline structure of the grown single crystals is orthorhombic. Long-range antiferromagnetic order sets in at temperatures below 22.5 K, while above this temperature the dependence of the magnetic susceptibility has a shape characteristic of interacting antiferromagnetic Heisenberg chains. We hypothesize that long-range magnetic order sets in below 22.5 K through the destruction of the ideal ladder structure of  $\text{LiCu}_2\text{O}_2$  because of partial redistribution of copper and lithium ions at the crystal lattice sites and because of the presence of other defects in the crystalline structure. © 1998 American Institute of Physics.  
[S1063-7761(98)02105-2]

### 1. INTRODUCTION

The discovery of high- $T_c$  superconductivity initiated a new stage in studies of oxocuprates, which are not superconductors but contain in their crystalline structure various fragments of Cu–O characteristic of high- $T_c$  superconductors. The oxocuprates  $\text{Bi}_2\text{CuO}_4$  and  $\text{CuGeO}_3$ , which were studied earlier,<sup>1–3</sup> in their stoichiometric state contain only bivalent ions  $\text{Cu}^{2+}$  in quadrant and octahedral oxygen surroundings, respectively.

The present paper is a first report on a study of magnetic and resonance properties of  $\text{LiCu}_2\text{O}_2$  single crystals. In contrast to  $\text{Bi}_2\text{CuO}_4$  and  $\text{CuGeO}_3$ , which contain only bivalent copper ions, in the  $\text{LiCu}_2\text{O}_2$  single crystal there are univalent and bivalent copper ions. The magnetic  $\text{Cu}^{2+}$  copper ions in this crystal are in pyramidal oxygen surroundings. These features determined our interest in studying the physical properties of  $\text{LiCu}_2\text{O}_2$  single crystals.

### 2. SAMPLES AND THE EXPERIMENTAL METHOD

The  $\text{LiCu}_2\text{O}_2$  single crystals were grown by slowly cooling the melt at a rate of 3–5 degrees per hour. The mixture for the melt consisted of  $\text{Li}_2\text{CO}_3$  and  $\text{CuO}$  in a 1.2-to-1 ratio. The mixture was placed in an alundum crucible, which in turn was placed inside a  $\text{ZrO}_2$  crucible. The temperature regime was chosen with allowance for dehydration of the reagents and for the decomposition of  $\text{Li}_2\text{CO}_3$  in the heating process. The peak temperature of the melt was 1150 °C. The time during which the melt was exposed to the peak temperature depended on the amount of mixture placed in the crucible, the size of the crucible, the size of the grains, and the extent to which the powders of the initial reagent could

be mixed, and amounted to about three to four hours. The crystals were shiny black plates occupying positions parallel to the surface of the fusing agent.

The crystals were drawn mechanically. The maximum dimensions of the crystals produced in this way were 3-by-4-by-1 mm.<sup>3</sup> Prolonged storage in the open air was found to lead to the formation of a mat coating on the crystal's surface.

Earlier x-ray studies of the samples<sup>4</sup> showed that the crystalline structure is orthorhombic with unit cell parameters  $a = 5.725 \text{ \AA}$ ,  $b = 2.857 \text{ \AA}$ , and  $c = 12.409 \text{ \AA}$ . These parameters coincide with the data of Ref. 5.

Magnetic susceptibility was measured by vibrating-reed and SQUID magnetometers in the temperature interval from 300 K to 4.2 K.

In our resonance measurements we used a magnetic-resonance spectrometer with a pulsed magnetic field with wavelength of 8 and 6 mm in the temperature interval from 300 K to 4.2 K. Magnetic resonance in the paramagnetic region was studied using an SE/X-2544 EPR spectrometer with  $\lambda = 3 \text{ cm}$ .

### 3. EXPERIMENTAL RESULTS

Figure 1 depicts the temperature curves for the magnetic susceptibility of  $\text{LiCu}_2\text{O}_2$  measured in an 80-Oe magnetic field along the  $c$  axis and along two mutually perpendicular directions in the  $ab$  plane. Estimates of the diamagnetic contribution and the Van Vleck susceptibility show that both contributions are smaller than the measured values by a factor of ten.

The susceptibility along the  $c$  axis is higher than in the other two directions over the entire temperature range. The

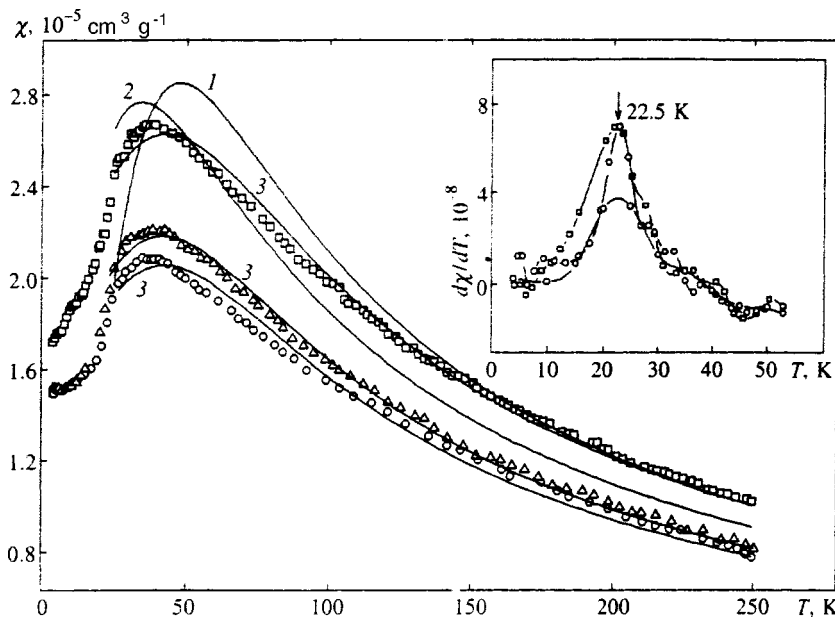


FIG. 1. Temperature curves for the magnetic susceptibility of  $\text{LiCu}_2\text{O}_2$ :  $\square$ — $\mathbf{H}\parallel\mathbf{c}$ , and  $\circ$  and  $\triangle$ — $\mathbf{H}\perp\mathbf{c}$ . The theoretical curves are denoted as follows: 1—alternatingly spaced magnetic chain, 2—two-dimensional Heisenberg model, and 3—one-dimensional model with interchain interaction. The inset depicts the temperature dependence of the first temperature derivatives of susceptibility.

high-temperature part of the reciprocal susceptibility is used to determine the values of the paramagnetic Néel temperatures in all three directions:

$$\Theta_c = -47 \text{ K}, \quad \Theta_{\perp 1} = -50 \text{ K}, \quad \Theta_{\perp 2} = -38 \text{ K}.$$

These values are lower than the value  $\Theta = -75 \text{ K}$  for polycrystalline  $\text{LiCu}_2\text{O}_2$  given in Ref. 6. The corresponding values of the effective magnetic moment are

$$\mu_c = 2.01\mu_B, \quad \mu_{\perp 1} = 1.83\mu_B, \quad \mu_{\perp 2} = 1.76\mu_B,$$

which are close to the theoretical value of  $1.73\mu_B$  for  $\text{Cu}^{2+}$ .

Figure 2 depicts the field curves for magnetization measured at 4.2 K along the  $\mathbf{c}$  axis and along two mutually perpendicular directions in the  $ab$  plane. All three curves represent a linear dependence up to 15 kOe. No residual magnetic moment or hysteresis phenomena were detected.

The results of studies of the temperature dependence of the EPR linewidth for three orientations of the magnetic field (along the  $\mathbf{c}$  axis and in the  $ab$  plane) are depicted in Fig. 3. As the temperature lowers, the EPR linewidth sharply increases as  $T$  approaches  $T \approx 30 \text{ K}$ . Below this temperature, no EPR signal was detected with the magnetic field directed along the  $\mathbf{c}$  axis. When the field was parallel to the  $ab$  plane, below  $T \approx 30 \text{ K}$  we observed resonant absorption, whose in-

tensity was found to diminish as the temperature was lowered still further. Below 15 K this resonance signal was not detected.

The angular curves for the EPR linewidth measured at room temperature are depicted in Fig. 4. When the magnetic field rotates in the  $ab$  plane, the linewidth varies sinusoidally with a period of  $\pi/2$ . When the magnetic field rotates in a plane perpendicular to the  $ab$  plane, the function  $A + B(1 + \cos^2\theta)$  provides a good description of the angular dependence of  $\Delta H$ , with the fitting parameters  $A$  and  $B$  depending on the orientation of this plane in relation to the crystallographic axes in the  $ab$  plane.

The temperature curves for EPR fields with both field orientations are depicted in Fig. 5. Figure 6 depicts the angular curves for the  $g$  factors measured at room temperature. For  $\mathbf{H}\parallel\mathbf{c}$  we have  $g_c = 2.225$ , while in the  $ab$  plane the  $g$  factor slowly varies sinusoidally with a period of  $\pi/2$  and extremal values 2.00 and 1.95.

Figure 7 depicts the frequency vs. field dependence of magnetic resonance, measured at  $T = 4.2 \text{ K}$  in  $\mathbf{H}\parallel\mathbf{c}$ . The dashed straight line shows the linear dependence  $\nu = \gamma H$ , where  $\gamma$  corresponds to the value  $g_c$  measured at room tem-

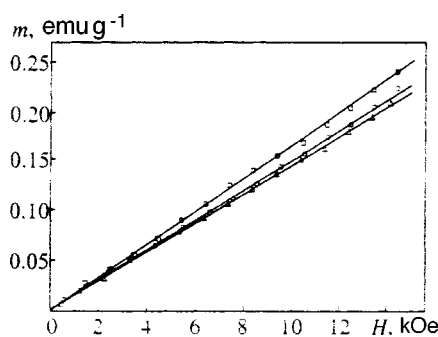


FIG. 2. Field curves for the magnetization of  $\text{LiCu}_2\text{O}_2$  at  $T = 4.2 \text{ K}$ :  $\square$ — $\mathbf{H}\parallel\mathbf{c}$ , and  $\circ$  and  $\triangle$ — $\mathbf{H}\perp\mathbf{c}$ .

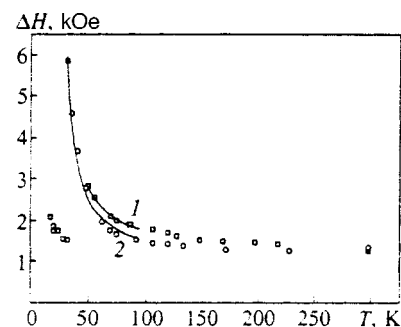


FIG. 3. Temperature curves for the EPR linewidth in  $\text{LiCu}_2\text{O}_2$  at  $\nu = 9.4 \text{ GHz}$ : 1—field  $\mathbf{H}$  is parallel to the  $ab$  plane, 2— $\mathbf{H}\parallel\mathbf{c}$ . The solid curves represent the results of power-law calculations.

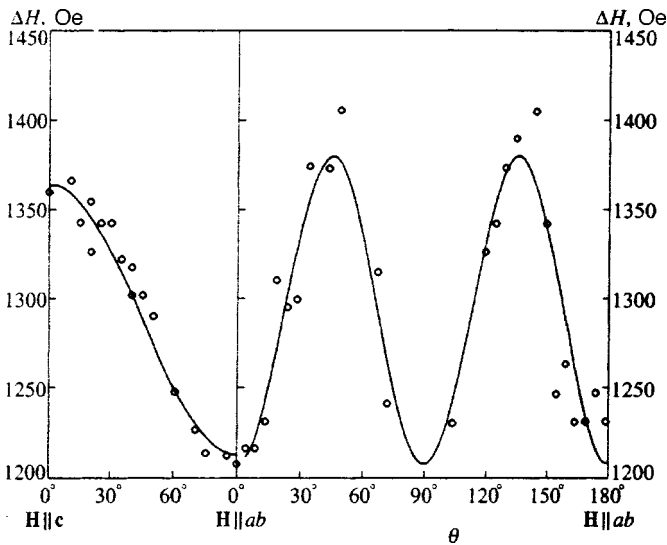


FIG. 4. Angular curves for the EPR linewidth in  $\text{LiCu}_2\text{O}_2$  at room temperature at  $\nu = 9.4$  GHz.

perature. The frequency vs. field dependence has a gap and is described by the polynomial

$$\nu = \nu_c + aH + bH^2, \tag{1}$$

where  $\nu_c = 29.83$  GHz,  $a = 0.5754$  GHz kOe $^{-1}$ , and  $b = 0.0265$  GHz kOe $^{-2}$ . Note that the frequency vs. field dependence does not asymptotically approach the linear dependence  $\nu = \gamma H$  as the field becomes stronger; it intersects this linear dependence at  $H \approx 13$  kOe.

We measured the temperature behavior of the resonance fields in  $\mathbf{H}||c$  at two frequencies, 44.61 and 46.27 GHz. Under the assumption that the coefficients  $a$  and  $b$  in Eq. (1) are temperature-independent, we calculated the temperature dependence of  $\nu_c$  (Fig. 8). According to this dependence, the  $\nu_c(T)$  curve is approximately equal to zero at  $T \approx 23$  K.

Figure 9 depicts the results of measuring the angular curves for the resonance field when the magnetic field is rotated in two mutually perpendicular planes containing the  $c$  axis. Within experimental error, both curves coincide. For the magnetic field in the  $ab$  plane the resonance field sharply increases, which made it impossible to measure the frequency vs. field dependence for this orientation.

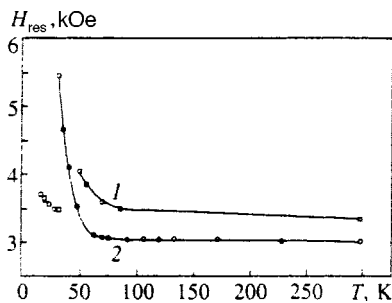


FIG. 5. Temperature curves for the EPR field in  $\text{LiCu}_2\text{O}_2$  at  $\nu = 9.4$  GHz: 1— $\mathbf{H}||ab$ , and 2— $\mathbf{H}||c$ .

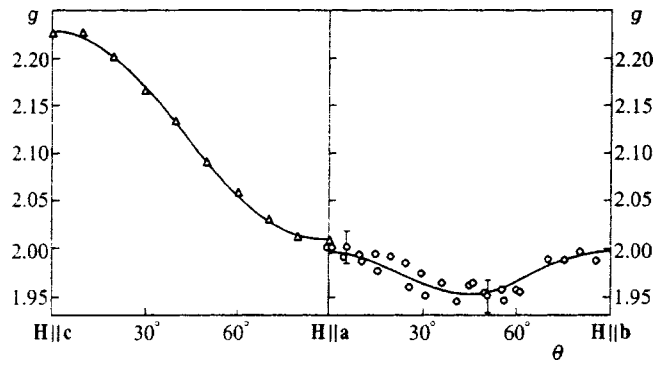


FIG. 6. Angular curves for the  $g$  factor of  $\text{LiCu}_2\text{O}_2$  at room temperature and  $\nu = 9.4$  GHz.

4. DISCUSSION

The crystalline structure of  $\text{LiCu}_2\text{O}_2$  was determined by Hibble *et al.*<sup>6</sup> by the x-ray method. They interpreted the structure  $\text{LiCu}_2\text{O}_2$  as tetragonal with the space group  $P4_2/nmc$  and  $a = 5.714$  Å and  $c = 12.401$  Å. Later, however, Berger *et al.*<sup>5</sup> interpreted the crystalline structure of  $\text{LiCu}_2\text{O}_2$  as orthorhombic with the space group  $Pnma$  and the unit cell parameters  $a = 5.72$  Å,  $b = 2.86$  Å, and  $c = 12.4$  Å. They explain why Hibble *et al.*<sup>6</sup> inferred tetrahedral symmetry in  $\text{LiCu}_2\text{O}_2$  by pointing out that  $a = 2b$ , so that there is crystal twinning, and this causes the x-ray spectra to have quasitetragonal symmetry. In Ref. 6 it was assumed that depending on the rate of melt cooling and other conditions of synthesis, the crystal symmetry may be either tetragonal or orthorhombic. Thus, the difference in determining the space group of the  $\text{LiCu}_2\text{O}_2$  crystal may be due to the different origin of the samples.

The crystalline structure of  $\text{LiCu}_2\text{O}_2$  with orthorhombic symmetry is depicted in Fig. 10a. The  $\text{Cu}^{2+}$  ions are at the base of the pyramid consisting of oxygen ions and are connected into chains along the  $\mathbf{b}$  axis of the crystal. The magnetic structure of  $\text{LiCu}_2\text{O}_2$  in this case is formed by two exchange-coupled chains of  $\text{Cu}^{2+}$  ions oriented along the  $\mathbf{b}$  axis of the crystal and belonging to two neighboring atomic planes that are perpendicular to the  $\mathbf{c}$  axis of the crystal. These planes form a layer in which the adjacent exchange-coupled pairs of chains consisting of copper ions are far from

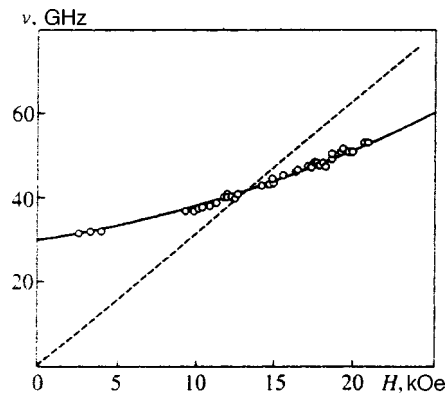


FIG. 7. Frequency vs. field dependence of the AFMR signal in  $\text{LiCu}_2\text{O}_2$  at  $T = 4.2$  K in  $\mathbf{H}||c$ . The solid curve represents the theoretical curve corresponding to Eq. (1).

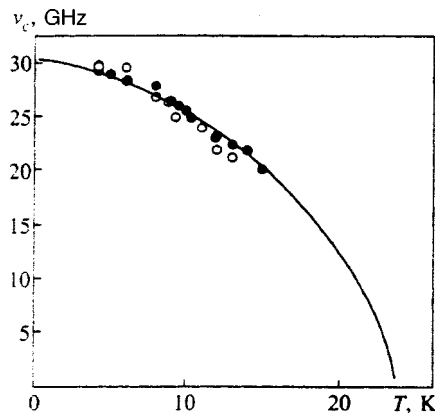


FIG. 8. Temperature curve for the AFMR gap in  $\text{LiCu}_2\text{O}_2$ :  $\circ$ — $\nu = 44.61$  GHz, and  $\bullet$ — $\nu = 46.27$  GHz.

each other and are separated by chains consisting of lithium ions also oriented along the **b** axis. Each layer is separated from a neighboring layer of the same kind by a plane containing nonmagnetic  $\text{Cu}^+$  ions. Thus, we have described a magnetic structure consisting of isolated pairs of exchange-coupled chains of  $\text{Cu}^{2+}$  ions, with a fragment shown in Fig. 10b.

Such magnetic structures are known in the literature as ladder systems,<sup>7</sup> and lately there has been an upsurge of interest in these structures. A ladder system consisting of two chains, or a two-leg ladder, is described by two exchange interactions, the intrachain interaction and the interchain interaction. In our case, as Fig. 10b clearly shows, we must introduce three exchange interactions to describe the magnetic structure. A similar structure was observed in the  $\text{KCuCl}_3$  crystal by Tanaka *et al.*,<sup>8</sup> who found that such a magnetic structure is a ladder system.

If there is twinning of the orthorhombic crystal, the crystal becomes divided into domains in such a way that in neighboring domains the crystallographic **b** axes are turned through  $90^\circ$  in relation to each other. However, in this case too the magnetic structure within a single domain is a ladder one. Since in crystal twinning the domains are usually macroscopic, the magnetic structure of the crystal as a whole can also be considered a ladder system.

When the symmetry is tetragonal, the crystalline structure of  $\text{LiCu}_2\text{O}_2$  proposed by Hibble *et al.*<sup>6</sup> differs from the orthorhombic in that in two neighboring atomic planes the

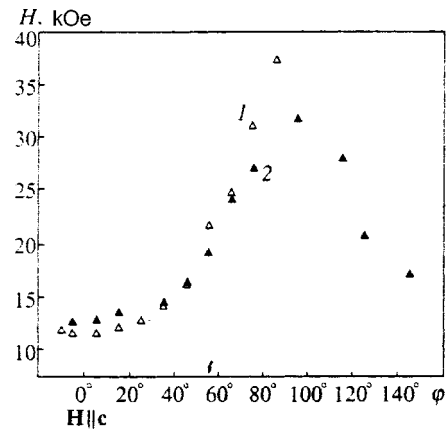


FIG. 9. Angular curves for the resonance field of the AFMR signal in  $\text{LiCu}_2\text{O}_2$  at  $T = 4.2$  K and  $\nu = 41.62$  GHz. The data 1 and 2 were obtained as a result of rotating the sample in two mutually perpendicular planes containing the **c** axis of the crystal.

ion copper chains are perpendicular to each other. In this case the magnetic structure is not a ladder one; more likely, it forms a two-dimensional system that is a bulk “lattice” of exchange-coupled chains consisting of neighboring atomic planes.

Thus, depending on the type of structure (orthorhombic or tetragonal) and the strength of the exchange coupling between the chains,  $\text{LiCu}_2\text{O}_2$  can be in the form of the following magnetic structures: noninteracting magnetic chains, exchange-coupled pairs of magnetic chains, or a two-dimensional magnetic structure consisting of two neighboring atomic planes with the chains in these planes perpendicular to each other.

Since x-ray studies of our samples of  $\text{LiCu}_2\text{O}_2$  confirmed the orthorhombic symmetry of the crystal, below we discuss the various magnetic structures that can arise in this case.

As shown in Refs. 7–10, the ground state of a ladder system with  $S = 1/2$  is nonmagnetic and is characterized by an energy gap between the ground and excited magnetic states. The presence of such a gap leads to a situation in which the magnetic susceptibility drops exponentially to zero as the temperature falls below a certain critical value.

The temperature curves for the susceptibility depicted in Fig. 1 do not exhibit the low-temperature exponential drop characteristic of ladder systems. More than that, the peaks in

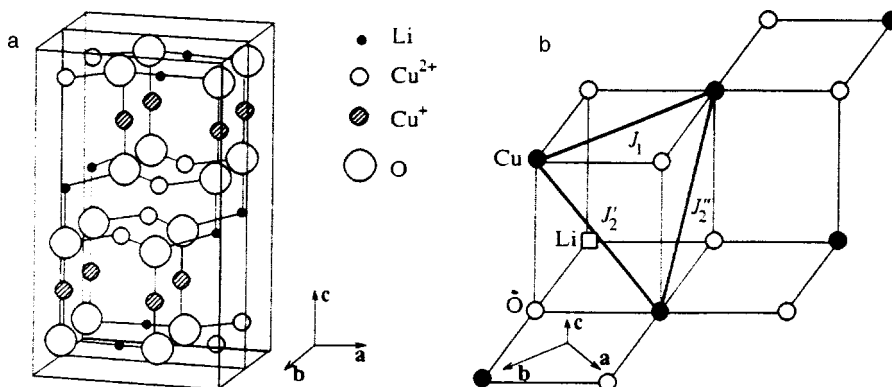


FIG. 10. (a) The crystalline structure of  $\text{LiCu}_2\text{O}_2$  with orthorhombic symmetry (according to the data of Ref. 5). (b) A fragment of the crystalline structure of  $\text{LiCu}_2\text{O}_2$  illustrating exchange interactions.

the first temperature derivatives for all three direction of the magnetic field at  $T=22.5$  K (the inset in Fig. 1) suggest that long-range magnetic order sets in below this temperature, which is assumed to be the Néel temperature  $T_N$ . Presumably, the existence of long-range magnetic order is also supported by the presence of a gap in the magnetic resonance spectrum at temperatures below 22.5 K (Figs. 7 and 8). The presence of magnetic order in the crystal suggests that there is no need to examine in detail the case of noninteracting magnetic chains.

Strictly speaking, the absence of an exponential drop in susceptibility makes it impossible to reject with certainty the ladder nature of the magnetic structure of  $\text{LiCu}_2\text{O}_2$ . Fukuyama *et al.*<sup>11</sup> studied the ladder system  $\text{SrCu}_2\text{O}_3$  and found that zinc ion impurities and, probably, other structural defects can give rise to a magnetic phase and, at sufficiently high concentrations of such defects, to the formation of a Néel state. According to Watanabe *et al.*,<sup>10</sup> strong anisotropy of the exchange interaction in a chain can also lead to such a state.

The presence of a broad maximum in the temperature curve for the susceptibility and the inequality  $T_N/T_{\chi\text{max}} = 0.59 < 1$  indicate that the magnetic structure of  $\text{LiCu}_2\text{O}_2$  is low-dimensional, with the antiferromagnetic interaction in a chain realized through a  $90^\circ$  bond. This situation is encountered in oxocuprates and, in particular, in  $\text{CuGeO}_3$ . It was given a theoretical basis by Geertsma and Khomskii.<sup>12</sup>

Figure 1 depicts the theoretical temperature curves for the susceptibility calculated in the two- and one-dimensional Bonner–Fisher models for planes and interacting antiferromagnetic Heisenberg chains.<sup>13,14</sup> Figure 1 also depicts the theoretical temperature curve for the magnetic susceptibility of an alternately spaced magnetic chain, whose behavior is similar to that of a ladder system.<sup>15</sup> The best agreement with experiment is achieved for a system of interacting antiferromagnetic chains with  $J_1 = -31.5$  K and  $|J_2| = 0.06$  K with the external magnetic field  $\mathbf{H}$  parallel to the  $c$  axis (here  $J_1$  and  $J_2$  are the intra- and interchain exchange integrals). The value of the intrachain exchange interaction  $J_1$ , estimated from the relation  $T_{\chi\text{max}} = 1.32|J_1|S(S+1)$  (see Ref. 16), is  $|J_1| = 39.6$  K.

A comparison of the theoretical and experimental curves suggests that the magnetic structure in  $\text{LiCu}_2\text{O}_2$  is quasi-one-dimensional. The absence of an exponential decay in susceptibility to zero (a decay characteristic of ladder systems) in this case is probably due to the presence of defects in the sample, which destroy the purely ladder state.

The crystalline structure of  $\text{LiCu}_2\text{O}_2$  shows that the  $\text{Li}^+$  and  $\text{Cu}^{2+}$  ions have the same pyramidal oxygen surroundings. This probably facilitates the situation in which in some of the lithium and bivalent copper ions change places. The possibility of such redistribution is corroborated, for instance, by the fact that doping  $\text{CuMg}_2\text{O}_3$  with lithium ions leads to a uniform distribution of the impurity ions among the Cu and Mg positions,<sup>17</sup> while in  $\text{LiCu}_3\text{O}_3$  the Li and Cu ions are distributed among equivalent positions statistically.<sup>6</sup>

On the one hand, such redistribution of ions violates the homogeneity of the ladder structure but, on the other, an exchange coupling develops between isolated ladder pairs of

chains via the  $\text{Cu}^{2+}$  ions that have occupied the positions of lithium ions. When the number of such copper ions is sufficiently large, long-range magnetic order of the Néel type may set in at a finite temperature in the crystal,<sup>11</sup> and the temperature curve for magnetic susceptibility is described by the theoretical curve for interacting chains. Here by exchange interaction between chains we mean an average value of the exchange interactions between chains within a two-leg ladder and the interaction between ladder pairs via the copper ions introduced into the lithium chains.

Another fact that speaks in favor of partial redistribution of copper and lithium ions in  $\text{LiCu}_2\text{O}_2$  is that after hardening the samples from high temperatures, the resonance and magnetic properties undergo a considerable change (as shown by preliminary measurement). Here we have not excluded the possibility that the redistribution of cations may lead to formation of a tetragonal phase. The problem of how heat treatment affects the structural and magnetic properties of  $\text{LiCu}_2\text{O}_2$  requires a special study.

We cannot exclude the possibility that conduction electrons also participate in the formation of long-range magnetic order in  $\text{LiCu}_2\text{O}_2$ . Most likely, the presence of copper ions with different valencies leads to a situation in which the electrical resistivity of  $\text{LiCu}_2\text{O}_2$  at room temperature is roughly  $10^2\text{--}10^3\ \Omega\text{cm}$ , which is smaller by several orders of magnitude than in  $\text{CuGeO}_3$  or  $\text{Bi}_2\text{CuO}_4$ .

The frequency vs. field dependence of magnetic resonance at low temperatures and, in particular, the presence of a gap in the magnetic excitation spectrum (Fig. 7) and the temperature dependence of this gap (Fig. 8) also suggest that antiferromagnetic order sets in at temperatures lower than 22.5 K. However, the gap in the AFMR spectrum is extremely narrow for orthorhombic antiferromagnets. As is well known,<sup>18</sup> the size of the gap in the AFMR spectrum for an orthorhombic antiferromagnet is given by the following expression:

$$\nu_c = \gamma\sqrt{2H_E H'_a},$$

where  $H_E$  is the exchange field, and, depending on the orientation of the external magnetic field with respect to the crystallographic axis,  $H'_a$  is one of the two effective fields  $H_{a1}$  and  $H_{a2}$  describing the anisotropy of a biaxial antiferromagnet or the difference of these fields. A possible situation (at least in principle) is when  $H_{a1}$  and  $H_{a2}$  are close in value and their difference determines a small value of the energy gap. But in this case, too, the absence of significant anomalies in the field curves for magnetization in a field  $H_c = \sqrt{2H_E H'_a} \approx 11.8$  kOe due to a spin-flop transition remains unexplained.

On the other hand, the frequency vs. field dependence does not approach the linear dependence  $\nu = \gamma H$  asymptotically as the magnetic field strength grows, as was to be expected in orthorhombic antiferromagnets, but intersects it. A frequency vs. field dependence of this kind can be observed, for instance, in antiferromagnets with a triangular (noncollinear) magnetic structure.<sup>19</sup>

When the external magnetic field was at right angles to the  $c$  axis of the crystal, we were unable to measure the

frequency vs. field dependence at frequencies above 37 GHz because of a sharp increase in the resonance field. However, on the basis of the angular dependence of the resonance field of AFMR (Fig. 9) it can be assumed that the external magnetic field deviates from the  $\mathbf{c}$  axis of the crystal, the gap in the AFMR spectrum diminishes and the slope of the frequency vs. field curve decreases.

It is quite possible that all the unusual properties of AFMR are due to the formation of a noncollinear magnetic structure for  $T < T_N$ . Such a structure may develop because of frustration of the exchange interaction in the triangular bond configuration (see Fig. 10b).

The increase in the EPR linewidth with the temperature decreasing below  $\approx 80$  K (Fig. 3) is described by the theoretical formula  $\Delta H \propto [(T - T_N)/T_N]^{-n}$ . The best agreement with the experimental results is achieved at  $n = 1.28$  and  $n = 1.35$  for  $\mathbf{H} \parallel \mathbf{c}$  and  $\mathbf{H} \perp \mathbf{c}$ , respectively. These values of the critical indices are close to the values  $n = 1.1 - 1.2$  determined from experiments with the quasi-one-dimensional magnetic materials  $\text{CuCl}_2 \cdot 2\text{NC}_5\text{H}_5$ ,  $\text{CsNiCl}_3$ , and  $\text{RbNiCl}_3$  (see Refs. 20 and 21).

An analysis of linewidths and the values of  $g$  factors measured at room temperature (Figs. 4 and 6) suggests the following. The large value of  $\Delta H$  cannot be explained by dipole-dipole and effective exchange ( $J_{\text{eff}} \propto 3\Theta_N/2zS(S+1)$ ) interactions and is determined by the anisotropic exchange interaction. When the magnetic field changes its orientation from the  $\mathbf{c}$  axis to the  $ab$  plane,  $\Delta H$  and the  $g$ -factor exhibit a typical angular dependence,  $\propto A(1 + \cos^2\theta)$ . However, in the  $ab$  plane both are characterized by  $90^\circ$  periodicity, while in orthorhombic crystals this angular dependence has a  $180^\circ$  period and tetragonal crystals exhibit no such angular dependence, provided that we ignore contributions of higher-order exchange interactions. We believe that such discrepancy is due to crystal twinning, in which the crystallographic axes in neighboring domains are rotated about the  $\mathbf{c}$  axis through an angle of  $90^\circ$ .

## 5. CONCLUSION

Our study of the structural, magnetostatic, and resonance properties of  $\text{LiCu}_2\text{O}_2$  single crystals leads to the following conclusions.

The  $\text{LiCu}_2\text{O}_2$  compound is a quasi-low-dimensional magnetic material. At  $T = 22.5$  K, long-range antiferromagnetic order sets in in a  $\text{LiCu}_2\text{O}_2$  single crystal. It is hypothesized that the magnetic structure in the magnetically ordered phase is noncollinear.

Our experimental results have been interpreted on the basis of the assumption that the crystalline structure of the

samples is orthorhombic (the space group  $Pnma$ ). In an ideal crystalline structure of  $\text{LiCu}_2\text{O}_2$  the positions of the atoms predetermine a magnetic structure of a two-leg ladder. However, defects in the crystalline structure, among which the most probable are the partial redistribution of copper and lithium ions  $\text{Cu}^{2+}$  and  $\text{Li}^+$  in chains and the oxygen nonstoichiometry, destroy the singlet state (a state characteristic of ladder systems with spin  $S = 1/2$ ) and introduce long-range magnetic order in the system.

The authors are grateful to K. S. Aleksandrov and O. A. Bayukov for useful discussions in the course of writing the paper, to D. A. Velikanov for measuring magnetic susceptibility, and to N. I. Kiselev for measuring electrical resistivity. This work was made possible by a grant from the Krasnoyarsk Regional Scientific Fund (Grant No. 6F0004).

\*E-mail: gap@post.krascience.rssi.ru

- <sup>1</sup>G. A. Petrakovskii, K. A. Sablina, A. M. Vorotynov, V. N. Vasiliev, A. I. Kruglik, A. D. Balaev, D. A. Velikanov, and N. I. Kiselev, *Solid State Commun.* **79**, 317 (1991).
- <sup>2</sup>A. I. Pankrats, G. A. Petrakovskii, and K. A. Sablina, *Solid State Commun.* **91**, 121 (1994).
- <sup>3</sup>G. A. Petrakovskii, K. A. Sablina, A. M. Vorotynov, A. I. Kruglik, A. G. Klimenko, A. D. Balayev, and S. S. Aplesnin, *Zh. Éksp. Teor. Fiz.* **98**, 1382 (1990) [*Sov. Phys. JETP* **71**, 772 (1990)].
- <sup>4</sup>W. Paszkowicz, A. Vorotynov, K. Sablina, and G. Petrakovskii, in *Abs. Int. Conf. on X-Ray Powder Diffraction Analysis of Real Structure of Matter*, Slovakia, 1995, p. 68.
- <sup>5</sup>R. Berger, P. Onnerud, and R. Tellgren, *J. Alloys Compd.* **184**, 315 (1992).
- <sup>6</sup>S. J. Hibble, J. Kohler, and A. Simon, *J. Solid State Chem.* **88**, 534 (1990).
- <sup>7</sup>E. Dagotto, J. Riera, and D. Scalapino, *Phys. Rev. B* **45**, 5744 (1992).
- <sup>8</sup>H. Tanaka, K. Takatsu, W. Shiramura, and T. Ono, *J. Phys. Soc. Jpn.* **65**, 1945 (1996).
- <sup>9</sup>M. Azuma, Z. Hiroi, M. Takano, K. Ishida and Y. Kitaoka, *Phys. Rev. Lett.* **73**, 3463 (1994).
- <sup>10</sup>H. Watanabe, K. Nomura, and S. Takada, *J. Phys. Soc. Jpn.* **62**, 2845 (1993).
- <sup>11</sup>H. Fukuyama, N. Nagaosa, M. Saito, and T. Tamimoto, *J. Phys. Soc. Jpn.* **65**, 2377 (1996).
- <sup>12</sup>W. Geertsma and D. Khomskii, *Phys. Rev. B* **54**, 3011 (1996).
- <sup>13</sup>J. Bonner and M. E. Fisher, *Phys. Rev.* **135**, A640 (1964).
- <sup>14</sup>G. S. Rushbrook and P. J. Wood, *Mol. Phys.* **1**, 257 (1958).
- <sup>15</sup>W. E. Hatfield, *J. Appl. Phys.* **52**, 1985 (1981).
- <sup>16</sup>T. de Neef, *Phys. Rev. B* **13**, 4141 (1976).
- <sup>17</sup>W. Winkelmann, H. A. Graf, and N. H. Anderson, *Phys. Rev. B* **49**, 310 (1994).
- <sup>18</sup>E. A. Turov, *Physical Properties of Magnetically Ordered Crystals* [in Russian], Publishing House of the USSR Academy of Sciences, Moscow (1963), p. 165.
- <sup>19</sup>L. A. Prozorova, V. I. Marchenko, and Yu. V. Krasnyak, *JETP Lett.* **41**, 637 (1985).
- <sup>20</sup>Y. Ajiro, H. Matsukawa, and Y. Shuni-Ichi, *Phys. Lett. A* **72**, 367 (1979).
- <sup>21</sup>V. V. Velichko and E. A. Petrakovskaia, in *Proc. 1st Int. Conf. on Physics of Magnetic Materials*, Poland, 1980.

Translated by Eugene Yankovsky